Analyses of the magnetic properties of $Y_3Fe_{29-x}Ti_x$ and other associated compounds

1997 J. Phys.: Condens. Matter 9 1339

(http://iopscience.iop.org/0953-8984/9/6/017)

J. Phys.: Condens. Matter **9** (1997) 1339–1346. Printed in the UK PII: S0953-8984(97)76602-5

Analyses of the magnetic properties of $Y_3Fe_{29-x}Ti_x$ and other associated compounds

F M Yang†, Xiu-Feng Han†, F R de Boer‡ and H S Li§

† State Key Laboratory for Magnetism, Institute of Physics, Chinese Academy of Sciences, PO Box 603, Beijing 100080, People's Republic of China

‡ Van der Waals–Zeeman Laboratory, University of Amsterdam, Valckenierstraat 65, 1018 XE Amsterdam, The Netherlands

§ School of Physics, The University of New South Wales, Sydney, NSW 2052, Australia

Received 24 July 1996, in final form 29 October 1996

Abstract. The novel compound $Y_3Fe_{29-x}Ti_x$ has been successfully synthesized. Its x-ray pattern can be indexed with a monoclinic symmetry and the $A_{2/m}$ space group. Thermomagnetic analysis gives a magnetic ordering temperature of 400 K. The saturation magnetization of $Y_3Fe_{27.6}Ti_{1.4}$ at 4.2 K and room temperature are $52.1\mu_B$ FU^{-1} and $38.0\mu_B$ FU^{-1} and the anisotropy fields at 4.2 K and room temperature are 5.2 T and 1.7 T, respectively. A systematic analysis of the magnetic properties of novel compounds $R_3Fe_{29-x}Ti_x$ (R = Y, Ce, Pr, Nd, Sm, Gd, or Tb) at 4.2 K has been performed on the basis of their saturation magnetization. This suggests that the saturation magnetization of $R_3Fe_{29-x}Ti_x$ compounds with a low stabilizing element concentration can be calculated roughly from a combination of those of the rhombohedral or hexagonal R_2Fe_{17} and tetragonal $RFe_{12-x}Ti_x$ units in a ratio of 1:1.

1. Introduction

The novel ternary phase of the rare earth and iron intermetallic compounds (R–Fe) stabilized by a third element (T) has been discovered by Collocott *et al* [1], Ivanova *et al* [2], Scherbakova *et al* [3], Fuerst *et al* [4] and Cadogan *et al* [5]. The crystal structure and the precise stoichiometry of this new phase has been suggested to be a $Nd_3(Fe, Ti)_{29}$-type structure by Li *et al* [6] using x-ray powder diffraction (XRD). The $Nd_3(Fe, Ti)_{29}$-type structure is monoclinic with the $P2_1/c$ space group [6]. Hu and Yelon [7] refined the $Nd_3(Fe, Ti)_{29}$ structure by neutron powder diffraction and obtained the same results as suggested by Li *et al*. The subsequent work of Kalogirou *et al* [8] suggested that the $Nd_3(Fe, Ti)_{29}$-type structure can be described more accurately in the $A_{2/m}$ space group.

This new family of intermetallic compounds $R_3(Fe, T)_{29}$ (T is the stabilizing element) have attracted special attention, because the introduction of the interstitial atoms N and C led to remarkable improvements in their magnetic properties [3, 9–12]. As an example, the new interstitial nitride $Sm_3(Fe, Ti)_{29}N_y$ compound exhibits strong uniaxial anisotropy and high saturation magnetization, which is close to those of $Sm_2Fe_{17}N_{3-\delta}$ and $Nd(Fe_{1-x}Ti_x)_{12}N_{1-\delta}$ and may become a potential candidate for permanent magnet application. Up to now the magnetic properties of several $R_3(Fe, Ti)_{29}$ compounds have been investigated while there is still lacking a complete analysis of the magnetic properties in this system. Therefore, it is highly desirable to carry out a systematic study on the phase formation and the intrinsic magnetic properties of the novel compounds $R_3(Fe, Ti)_{29}$.

0953-8984/97/061339+08$19.50

In order to understand the properties of other novel compounds $R_3(Fe, Ti)_{29}$ (R = rare earth) a systematic investigation of the intrinsic magnetic properties of $Y_3(Fe, Ti)_{29}$ is important, which makes it possible to isolate the magnetic properties of the 3d sublattice for these compounds. Although the $Y_3(Fe, Ti)_{29}$ compound with a starting composition of $Y_9Fe_{86}Ti_5$ was obtained by Li *et al* [13], amount of the impurity 1:12 phase is about 20%; the exact saturation magnetization and anisotropy fields at 4.2 K and room temperature were not given. In this work, the novel compound $Y_3Fe_{29-x}Ti_x$ with good single-phase charactor was synthesized. From the magnetic properties of $Y_3Fe_{29-x}Ti_x$ a systematic investigation of the structural and magnetic properties of the novel compounds $R_3Fe_{29-x}Ti_x$ (R = Y, Ce, Pr, Nd, Sm, Gd or Tb) has been performed.

2. Sample preparation and experimental methods

Samples with the composition $Y_3Fe_{29-x}Ti_x$ were prepared by arc melting the constituent elements with a purity of at least 99.9% in an argon atmosphere. In order to compensate the loss of the Y during melting and annealing, a 5–10% excess of Y relative to the ideal $Y_3Fe_{29-x}Ti_x$ composition was added. The ingots were melted in the water-cooled copper hearth and remelted at least four times to ensure homogeneity. The ingots were subsequently annealed in a sealed quartz tube under a protective argon atmosphere at 1233 K for 3 d in order to maximize the amount of $Y_3Fe_{29-x}Ti_x$ phase. At the end of the anneal, the ingots were water quenched to avoid slow cooling.

XRD with Cu Kα radiation was used to identify the phase of the alloys and to calculate the lattice parameters. A thermomagnetic analysis (TMA) using a vibrating-sample magnetometer (VSM) in the temperature range from 4.2 K to above the Curie temperature in a low field of about 0.04 T was used to judge the single-phase characteristics and to determine the Curie temperature T_C. XRD of the magnetically aligned powder samples was also used to determine the easy-magnetization direction of the compound.

3. Results and discussion

The composition of the $Y_3Fe_{27.6}Ti_{1.4}$ compound is deduced from an energy spectrum analysis in the scanning electron microscope based on the stoichiometric composition. Figure 1 shows the XRD pattern of the $Y_3Fe_{27.6}Ti_{1.4}$ compound. This pattern was indexed in the monoclinic $Nd_3(Fe, Ti)_{29}$-type structure with the $A_{2/m}$ space group and is as shown in figure 1. The lattice parameters of $Y_3Fe_{27.6}Ti_{1.4}$ were deduced from this pattern as given in table 1, together with the lattice parameters of other $R_3Fe_{29-x}Ti_x$ (R = Ce, Pr, Nd, Sm, Gd or Tb) compounds.

Figure 2 shows the magnetization as a function of temperature for an isotropic polycrystalline sample of $Y_3Fe_{27.6}Ti_{1.4}$, measured with a VSM in the temperature range from 4.2 K to above the Curie temperature in a low field of 0.046 T. It can be seen that the dominant phase is 3:29 except for a small amount of $Y(Fe, Ti)_{12}$ and α-Fe as impurity phases which were confirmed by the TMA in addition to the XRD. The Curie temperature T_C of $Y_3Fe_{27.6}Ti_{1.4}$ was derived by plotting M^2 versus T curves and extrapolating M to zero.

To examine the amount of impurity phases in the sample the magnetization as a function of temperature was measured in a field of 1.2 T on loose powder samples of $Y_3Fe_{27.6}Ti_{1.4}$, which were free to orient in the applied magnetic field in a magnetic balance in the temperature range from 77 to 1200 K as shown in figure 3. It can be seen that the main

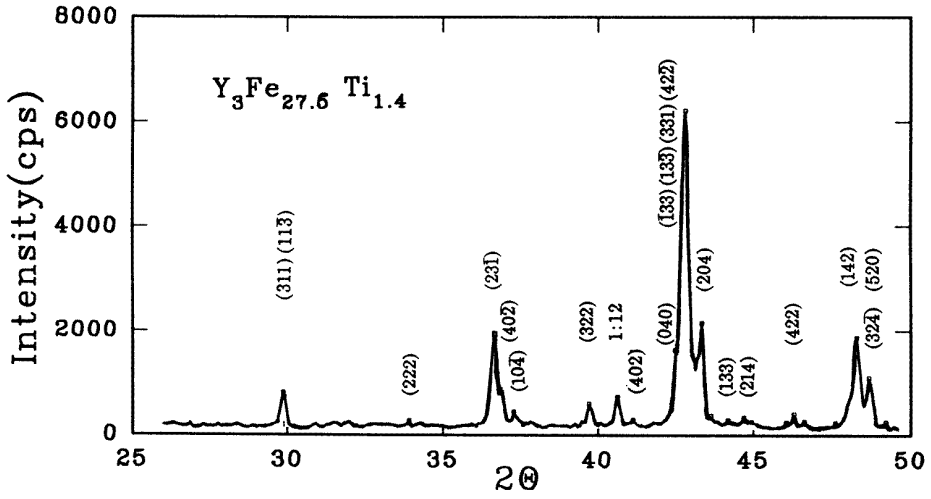

Figure 1. XRD patterns with Cu Kα radiation for $Y_3Fe_{27.6}Ti_{1.4}$.

Table 1. The lattice parameters a, b, c and β, the unit-cell volume $V = abc\sin\beta$ derived from the analysis of x-ray data with the monoclinic symmetry and the x-ray density ρ derived from the lattice constants for $R_3Fe_{29-x}Ti_x$ (R = Y, Ce, Pr, Nd, Sm, Gd or Tb) compounds.

$R_3Fe_{29-x}Ti_x$	a (Å)	b (Å)	c (Å)	β (deg)	V (Å^3)	ρ (g cm^{-3})	Reference
$Y_3Fe_{27.6}Ti_{1.4}$	10.56	8.50	9.68	96.76	862.5	7.22	This work
$Y_3Fe_{29-x}Ti_x$	10.61	8.52	9.69	97.15	869.4		[13]
$Ce_3Fe_{27.4}Ti_{1.6}$	10.56	8.49	9.68	96.7	862.	7.81	[4]
$Pr_3Fe_{27.6}Ti_{1.4}$	10.63	8.59	9.74	96.89	882.9	7.64	[18]
$Pr_3Fe_{27.5}Ti_{1.5}$	10.64	8.63	9.76	97.1	890	7.58	[4]
$Nd_3Fe_{27.8}Ti_{1.2}$	10.62	8.58	9.73	96.91	880.1	7.71	[18]
$Nd_3Fe_{27.7}Ti_{1.3}$	10.64	8.59	9.76	96.92	884.9	7.66	[14]
$Nd_3Fe_{27.6}Ti_{1.4}$	10.66	8.57	9.75	96.85	884.5	7.66	This work
$Nd_3Fe_{27.4}Ti_{1.6}$	10.65	8.59	9.75	96.9	885.5	7.65	[4]
$Sm_3Fe_{27.8}Ti_{1.2}$	10.63	8.57	9.72	97.0	878.9	7.79	[4]
$Sm_3Fe_{27.1}Ti_{1.9}$	10.65	8.58	9.72	97.0	881.6	7.74	[9]
$Sm_3Fe_{27.0}Ti_{2.0}$	10.62	8.56	9.72	96.97	877.1	7.78	[18]
$Gd_3Fe_{28.4}Ti_{0.6}$	10.62	8.51	9.70	97.04	870.0	7.96	[15]
$Tb_3Fe_{27.8}Ti_{1.2}$	10.58	8.51	9.67	97.02	864.9	8.01	[16]

contribution of impurity phases to the saturation magnetization at high temperatures is from α-Fe, and the impurity $Y(Fe, Ti)_{12}$ phase in the sample can be neglected. It is well known that the saturation magnetization values of pure iron (BCC Fe) at 4.2 K and room temperature are 221.7 A m^2 kg^{-1} and 217.2 A m^2 kg^{-1}, respectively, and the values of saturation magnetization of pure iron can be roughly thought to be constant in the temperature range from 4.2 K to room temperature. So it can be approximately considered that the saturation magnetization contributed by the α-Fe impurity phase at 4.2 K and room temperature have the same value, 20 A m^2 kg^{-1}, derived from M versus T plots by extrapolating T from a high temperature (500–700 K) to 4.2 K in figure 3. The additional increase in saturation magnetization of the impurity α-Fe phases in the sample in the temperature range from 800

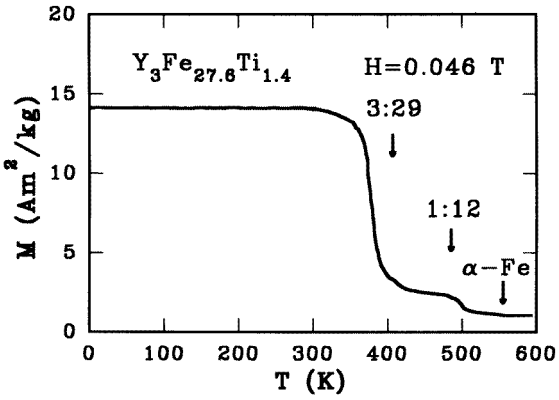

Figure 2. Thermomagnetic curves for the isotropic polycrystalline $Y_3Fe_{27.6}Ti_{1.4}$ samples in a low field of about 0.046 T.

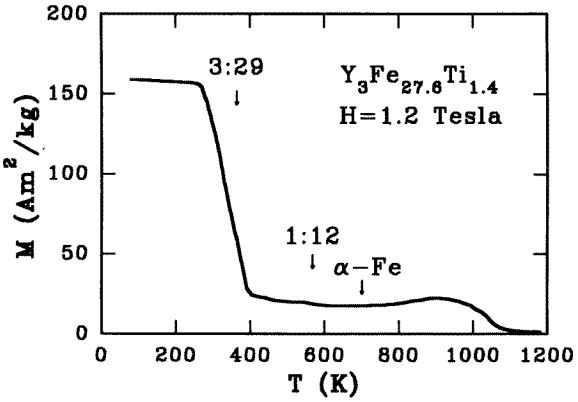

Figure 3. Thermomagnetic curves for the free powder samples of $Y_3Fe_{27.6}Ti_{1.4}$ in a field of 1.2 T.

to 1000 K probably resulted from decomposition of the small amount of sub-steady-state phase $Y_3Fe_{29-x}Ti_x$ and separating out some α-Fe from the powder samples. The amount of α-Fe impurity phases in the sample was derived to be about 9 wt%, deduced from (20 A m^2 kg^{-1})/(221.7 A m^2 kg^{-1}).

In order to prepare magnetically aligned samples the finely powdered particles were mixed with epoxy resin and placed in a plastic tube of cylindrical shape. For a non-spinning sample the plastic tube was placed in an applied magnetic field of about 1.2 T with the cylindrical axis parallel to the field direction and for a spinning sample the plastic tube was connected to a motor that drives the tube to spin in an applied magnetic field of about 1.2 T with the cylindrical axis perpendicular to the field direction until the epoxy resin solidified. The former is suitable for a material with uniaxial anisotropy whereas the latter is suitable for a material with planar anisotropy. Figure 4 shows the magnetic isotherms of the magnetically aligned samples of $Y_3Fe_{27.6}Ti_{1.4}$ at 4.2 K measured with a VSM in an external field up to 7 T applied parallel and perpendicular to the alignment direction, i.e. the easy axis of the sample. The anisotropy field B_a at 4.2 K was determined

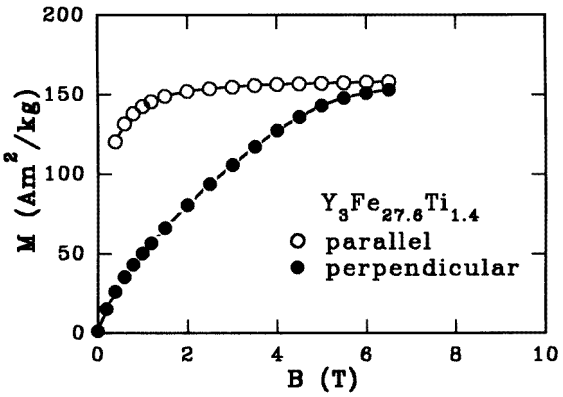

Figure 4. Isotherms at 4.2 K for $Y_3Fe_{27.6}Ti_{1.4}$ with the external field applied either parallel or perpendicular to the alignment direction of the cylinder samples.

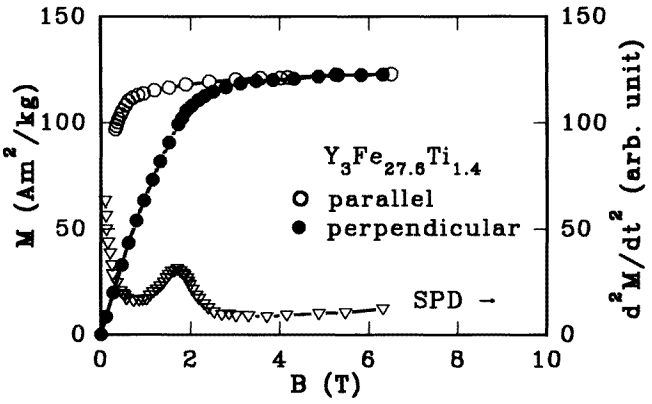

Figure 5. Isotherms and SPD signals at room temperature for $Y_3Fe_{27.6}Ti_{1.4}$ with the external field applied either parallel or perpendicular to the alignment direction of the cylinder samples.

from the intersection of the two magnetization curves measured with the magnetic field applied parallel and perpendicular, respectively, to the alignment direction of the cylindrical samples.

Figure 5 illustrates the magnetic isotherms of the magnetically aligned samples of $Y_3Fe_{27.6}Ti_{1.4}$ at room temperature measured in a pulsed magnetic field (PMF) together with the singular point detection (SPD) signal plots (dM^2/dt^2 versus B) measured by the SPD technique [17]. Singularity in the SPD signal corresponds to the anisotropy field B_a.

The saturation magnetization of $Y_3Fe_{27.6}Ti_{1.4}$ at 4.2 K and at room temperature were derived from the M versus $1/B$ plots by extrapolating $1/B$ to zero based on the high-field data of magnetization curves measured at 4.2 K and at room temperature in the external field applied parallel to the alignment direction of the cylinder samples. After deducing the contribution of the α-Fe impurity phase the saturation magnetization of $Y_3Fe_{27.6}Ti_{1.4}$ was derived to be 155.2 A m^2 kg^{-1} (52.1μ_B FU^{-1}) at 4.2 K, which corresponds to an average iron magnetic moment of 1.89μ_B/Fe atom and 113.2 A m^2 kg^{-1} (38.0μ_B FU^{-1}) at room temperature.

The intrinsic magnetic property parameters including the Curie temperature T_C, the saturation magnetization M_S and the anisotropy field B_a at 4.2 K and room temperature of $Y_3Fe_{27.6}Ti_{1.4}$ and $R_3Fe_{29-x}Ti_x$ (R = Ce, Pr, Nd, Sm, Gd or Tb) are given in table 2. It can be seen that the Curie temperature of $R_3Fe_{29-x}Ti_x$ increases with increasing atomic number of the rare earth from R = Ce to Gd and decreases from R = Gd to Tb. $Gd_3Fe_{28.4}Ti_{0.6}$ has the highest Curie temperature of 517 K. From table 2 it can also be seen that the saturation magnetization of $R_3Fe_{29-x}Ti_x$ at 4.2 K decreases gradually with increasing atomic number of the rare earth from R = Pr to Gd; $Ce_3Fe_{27.4}Ti_{1.6}$ is an exception.

Table 2. Curie temperature T_C, the saturation magnetization M_S and the anisotropy field B_a at 4.2 K and room temperature (RT) of $R_3Fe_{29-x}Ti_x$ (R = Y, Ce, Pr, Nd, Sm, Gd or Tb) compounds.

$R_3Fe_{29-x}Ti_x$	T_C (K)	M_S (4.2 K) (μ_B FU^{-1})	M_S (RT) (μ_B FU^{-1})	B_a (4.2 K) (T)	B_a (RT) (T)	Reference
$Y_3Fe_{27.6}Ti_{1.4}$	400	52.1	38.0	5.2	1.7	This work
$Y_3Fe_{29-x}Ti_x$	386					[13]
$Ce_3Fe_{27.4}Ti_{1.6}$	322	47.0	31.4	—	—	[4]
$Pr_3Fe_{27.6}Ti_{1.4}$	373	56.4[a]	46.2	6.3[a]	4.0	[18]
$Pr_3Fe_{27.5}Ti_{1.5}$	393	60.7	45.4	—	—	[4]
$Nd_3Fe_{27.8}Ti_{1.2}$	396	58.2[a]	47.6	9.8[a]	7.7	[18]
$Nd_3Fe_{27.7}Ti_{1.3}$	411	57.3	48.6	—	—	[14]
$Nd_3Fe_{27.6}Ti_{1.4}$	428	57.8	—	—	—	This work
$Nd_3Fe_{27.5}Ti_{1.5}$	424	58.9	44.5	—	—	[19]
$Nd_3Fe_{27.4}Ti_{1.6}$	419	58.5	44.8	—	—	[4]
$Sm_3Fe_{27.8}Ti_{1.2}$	469	51.6	45.2	—	—	[4]
$Sm_3Fe_{27.1}Ti_{1.9}$	486	51.5	43.8	—	3.4	[9]
$Sm_3Fe_{27.0}Ti_{2.0}$	452	50.8[a]	43.6	7.8[a]	5.8	[18]
$Gd_3Fe_{28.4}Ti_{0.6}$	517	38.1	31.8	9.8	—	[15]
$Tb_3Fe_{27.8}Ti_{1.2}$	455	—	—	—	6.4	[16]

[a] These values were measured at 12 K.

4. Analyses of the calculation

The 3:29-type compounds with monoclinic symmetry and $A_{2/m}$ space group have an intermediate structure between the rhombohedral Th_2Zn_{17} (2:17R) and the tetragonal $ThMn_{12}$ (1:12) structures and consist of a combination of the 2:17R and 1:12 units in a ratio of 1:1. The 2:17, 3:29 and 1:12 structures can all be derived from the $CaCu_5$-type structure by different dumbbell substitutions [6, 20]. This indicates an intrinsic connection in the crystallographic properties among these compounds.

In order to examine the intrinsic relationship in the magnetic properties between the 2:17, 3:29 and 1:12-type compounds, a systematic analysis of the saturation magnetization of the three kinds of compound and their mutual relationship was carried out. On the assumption that $R_3Fe_{29-x}Ti_x$ consists of $R_2Fe_{17-x}Ti_x$ and RFe_{12} or R_2Fe_{17} and $RFe_{12-x}Ti_x$, the corresponding calculated saturation magnetizations at 4.2 K are expressed as $M_S^{cal}(1)$ and $M_S^{cal}(2)$, respectively. These are the two extreme conditions and the actual saturation magnetization M_S of the 3:29-type compound should be in between $M_S^{cal}(1)$ and $M_S^{cal}(2)$. In addition it is also supposed that the total magnetic moment of the Fe sublattice in R_2Fe_{17} is parallel to that in RFe_{12}, and the magnetic moment of the rare-earth sublattice in both R_2Fe_{17} and RFe_{12} is parallel to that of the Fe sublattice for R = light rare earth or perpendicular

for R = heavy rare earth. The magnetic moments (M_R) of the rare-earth ions were taken from [21, 22]. With the average iron magnetic moment M_{Fe} taken to be $2.01\mu_B$/Fe atom in Y_2Fe_{17} [23] and $1.687\mu_B$/Fe atom in $YFe_{11}Ti$ [24] the saturation magnetizations of the $R_3Fe_{29-x}Ti_x$ compounds were calculated and the results obtained are listed in table 3. The experimental values M_S^{exp} for $R_3Fe_{29-x}Ti_x$ are listed in table 3 for comparison. It can been seen that the calculated values M_S^{cal} for the $R_3Fe_{29-x}Ti_x$ (R = Y, Pr, Nd, Sm or Gd) compounds with a low stabilizing element concentration are approximately in agreement with the experimental results M_S^{exp}.

Table 3. The calculated saturation magnetization values $M_S^{cal}(1)$, $M_S^{cal}(2)$ (in the two extreme cases) and $M_S^{cal}(3)$. In the calculation the average iron magnetic moment M_{Fe} of $1.89\mu_B$/Fe atom was taken from $Y_3Fe_{27.6}Ti_{1.4}$ for $R_3Fe_{29-x}Ti_x$ (R = Y, Ce, Pr, Nd, Sm, Gd or Tb) compounds at 4.2 K. The experimental values of the saturation magnetization M_S^{exp} of $R_3Fe_{29-x}Ti_x$ and the average iron magnetic moment M_{Fe}^{exp} of the $R_3Fe_{29-x}Ti_x$ which are taken from the saturation magnetization M_S^{exp}. The experimental data M_S^{exp} in [18] were measured at 12 K.

$R_3Fe_{29-x}Ti_x$	M_R (μ_B/R atom)	$M_S^{cal}(1)$ (μ_B FU^{-1}), $R_2Fe_{17-x}Ti_x+RFe_{12}$	$M_S^{cal}(2)$ (μ_B FU^{-1}), $R_2Fe_{17}+RFe_{12-x}Ti_x$	$M_S^{cal}(3)$ (μ_B FU^{-1}), $R_3Fe_{29-x}Ti_x$	M_S^{exp} (μ_B FU^{-1}), $R_3Fe_{29-x}Ti_x$	M_{Fe}^{exp} (μ_B/Fe atom), $R_3Fe_{29-x}Ti_x$
$Y_3Fe_{27.5}Ti_{1.5}$	0	51.6	52.1		52.1	1.89
$Ce_3Fe_{27.4}Ti_{1.6}$					47.0 [4]	
$Pr_3Fe_{27.6}Ti_{1.4}$	2.3	58.4	58.9	59.0	56.4 [18]	1.80
$Pr_3Fe_{27.5}Ti_{1.5}$	2.3	58.3	58.8	58.9	60.7 [4]	1.96
$Nd_3Fe_{27.8}Ti_{1.2}$	2.4	59.2	59.6	59.7	58.2 [18]	1.83
$Nd_3Fe_{27.7}Ti_{1.3}$	2.4	59.0	59.4	59.5	57.3 [14]	1.81
$Nd_3Fe_{27.6}Ti_{1.4}$	2.4	58.8	59.2	59.4	57.8	1.83
$Nd_3Fe_{27.5}Ti_{1.5}$	2.4	58.6	59.1	59.2	58.9 [19]	1.88
$Nd_3Fe_{27.4}Ti_{1.6}$	2.4	58.4	58.9	59.0	58.5 [4]	1.87
$Sm_3Fe_{27.8}Ti_{1.2}$	0.4	53.2	53.6	53.7	51.6 [4]	1.81
$Sm_3Fe_{27.1}Ti_{1.9}$	0.4	51.8	52.4	52.4	51.5 [9]	1.86
$Sm_3Fe_{27.0}Ti_{2.0}$	0.4	51.6	52.2	52.2	50.8 [18]	1.84
$Gd_3Fe_{28.4}Ti_{0.6}$	7.0	32.2	32.4	32.7	38.1 [15]	2.08
$Tb_3Fe_{27.8}Ti_{1.2}$	9.0	25.0	25.4	25.5	—	—

The saturation magnetization values of the $R_3Fe_{29-x}Ti_x$ compounds can also be calculated from the magnetic moment of the constituted elements. Using the formulae $M_S^{cal}(3) = (29-x)M_{Fe}+3M_R$ for R = light rare earth and $M_S^{cal}(3) = (29-x)M_{Fe}-3M_R$ for R = heavy rare earth, where $M_{Fe} = 1.89\mu_B$/Fe atom which was taken from $Y_3Fe_{27.6}Ti_{1.4}$, the calculated values $M_S^{cal}(3)$ of $R_3Fe_{29-x}Ti_x$ at 4.2 K are obtained and listed in table 3. These calculated values $M_S^{cal}(3)$ also approach the experimental results.

In table 3, the calculated value M_S^{cal} for $Ce_3Fe_{27.4}Ti_{1.6}$ was not given because the Ce ion is valence fluctuated and the magnetic moment of the Ce ion is difficult to determine precisely.

The average iron atomic magnetic moments of $R_3Fe_{29-x}Ti_x$ (R = Y, Pr, Nd, Sm, Gd or Tb) compounds were derived from $M_{Fe} = (M_S^{exp} - 3M_R)/(29-x)$ for R = light rare earth and $M_{Fe} = (M_S^{exp} + 3M_R)/(29-x)$ for R = heavy rare earth, as listed in table 3. It is shown that the average iron atomic magnetic moments of the $R_3Fe_{29-x}Ti_x$ compounds with a low stabilizing element concentration are close to that of Y_2Fe_{17}.

In conclusion the calculated saturation magnetizations $M_S^{cal}(1)$, $M_S^{cal}(2)$ and $M_S^{cal}(3)$ for $R_3Fe_{29-x}Ti_x$ (R = Y, Pr, Nd, Sm or Gd) compounds at 4.2 K are consistent with the experimental results M_S^{exp}. This suggests that the saturation magnetizations of $R_3Fe_{29-x}Ti_x$

compounds with a smaller stabilizing element concentration at 4.2 K can be roughly calculated from a combination of the saturation magnetization of the 2:17 and 1:12 units in a ratio of 1:1.

Acknowledgments

This project was supported by the National Natural Science Foundation of China and in part by the China Postdoctoral Science Foundation.

References

[1] Collocott S J, Day R K, Dunlop J B and Davis R L 1992 *Proc. 7th Int. Symp. on Magnetic Anisotropy and Coercivity in Rare-Earth–Transition Metal Alloys (Canberra, 1992)* ed Hi-Perm Laboratory, Research Center for Advanced Mineral and Material Procession, University of Western Australia, p 437
[2] Ivanova G V, Shcherbakova Ye V, Belozerov Ye V, Yermolenko A S and Teytel Ye I 1990 *Phys. Met. Metallorg: (USSR)* **70** 63
[3] Shcherbakova Ye V, Ivanova G V, Yermolenko A S, Belozerov Ye V and Gaviko V S 1992 *J. Alloys Compounds* **182** 199
[4] Fuerst C D, Pinkerton F E and Herbst J F 1994 *J. Appl. Phys.* **76** 6144
[5] Cadogan J M, Li H-S, Margarian A, Dunlop J B, Ryan D H, Collocott S J and Davis R L 1994 *J. Appl. Phys.* **76** 6138
[6] Li H-S, Cadogan J M, Xu J-M, Dou S X and Lin H K 1993 *Proc. Int. Conf. on the Application of the Mössbauer Effect (Vancouver, 1993)* paper 15-29B
Li H-S, Cadogan J M, Xu J-M, Dou S X and Lin H K 1994 *Hyperfine Interactions* **94** 1929
[7] Hu Z and Yelon W B 1994 *J. Appl. Phys.* **76** 6147
[8] Kalogirou O, Psycharis V, Saettas L and Niarchos D 1995 *J. Magn. Magn. Mater.* **145** 1
[9] Yang Fuming, Nasunjilegal B, Wang Jiangli, Zhu Jiangjun, Qin Weidong, Tang N, Zhao Ruwen, Bo-Ping Hu, Yi-Zhong Wang and Hong-Shou Li 1995 *J. Phys.: Condens. Matter* **7** 1679
[10] Ryan D H, Cadogan J M, Margarian A and Dunlop J B 1994 *J. Appl. Phys.* **76** 6150
[11] Bo-Ping Hu, Gui-Chuan Lui, Yi-Zhong Wang, Nasunjilegal B, Ru-Wen Zhao, Fu-Ming Yang, Hong-Shuo Li and Cadogan J M 1994 *J. Phys.: Condens. Matter* **6** L197
[12] Bo-Ping Hu, Gui-Chuan Lui, Yi-Zhong Wang, Nasunjilegal B, Ning Tang, Fu-Ming Yang, Hong-Shuo Li and Cadogan J M 1994 *J. Phys.: Condens. Matter* **6** L595
[13] Hong-Shuo Li, Courtois D, Cadogan J M, Xu J-M and Dou S X 1994 *J. Phys.: Condens. Matter* **6** L771
[14] Cadogan J M, Hong-Shuo Li, Davis R L, Margarian A, Dunlop J B and Gwan P B 1994 *J. Appl. Phys.* **75** 7114
[15] Nasunjilegal B, Yang Fuming, Zhu Jiangjun, Huayong Pan, Wang Jiangli, Qin Weidong, Ning Ting, Bo-Ping Hu, Yi-Zhong Wang, Hong-Shou Li and Cadogan J M 1996 *Acta Phys. Sin.* **5** 544
[16] Ibarra M R, Morellon L, Blasco J, Pareti L, Algarabel P A, Garcia J, Albertini F and Paoluzzi A 1994 *J. Phys.: Condens. Matter* **6** L771
[17] Asti G and Bolzoni F 1985 *J. Appl. Phys.* **58** 1924
[18] Margarin A, Dunlop J B, Colloctt S J, Li H-S, Cadogan J M and Davis R L 1994 *Proc. 8th Int. Symp. on Magnetic Anisotropy and Coercivity in R–T Alloys (Birmingham, 1994)*
[19] Fuerst C D, Pinkerton F E and Herbst J F 1994 *J. Magn. Magn. Mater.* **129** L115
[20] Johnson Q and Smith G S 1968 *Lawrence Radiation Laboratory Report* UCRL-71094
[21] Han Xiu-Feng, Jin Han-Min, Zhao T S and Sun C C 1993 *J. Phys.: Condens. Matter* **5** 8603
[22] Han Xiu-Feng, Jin Han-Min, Wang Zi-Jun, Sun C C and Zhao T S 1993 *Phys. Rev.* B **47** 3248
[23] Averbuch-Pouchot M T, Chevalier R, Deportes J, Kebe B and Lemaire R 1987 *J. Magn. Magn. Mater.* **68** 190
[24] Yingchang Yang 1995 *Proc. 3rd Int. Symp. on Physics of Magnetic Materials (Seoul, 1995)* vol 1 (The Korean Magnetics Society) p 6